Eur. Phys. J. A (2021) 57:265
https://doi.org/10.1140/epja/s10050-021-00563-z

THE EUROPEAN PHYSICAL JOURNAL A

Regular Article - Theoretical Physics

Froissaron and Maximal Odderon with spin-flip in pp and $\bar{p}p$ high energy elastic scattering

N. Bence[1,a], A. Lengyel[2,b], Z. Tarics[2,c], E. Martynov[3,d], G. Tersimonov[3,e]

[1] Uzhgorod National University, Universitetska Street 14, Uzhgorod 88017, Ukraine
[2] Institute of Electron Physics of NAS of Ukraine, Universytetska Street 21, Uzhgorod 88017, Ukraine
[3] Bogolyubov Institute for Theoretical Physics of NAS of Ukraine, Metrologichna street 14b, Kiev 03143, Ukraine

Received: 12 April 2021 / Accepted: 6 August 2021

Communicated by Reinhard Alkofer

Abstract The scattering amplitude with spin-non-fiip and spin-flip components represented by Froissaron, Maximal Odderon as well as by standard Regge poles contributions is considered. From the fit to the data of pp and $\bar{p}p$ scattering at high energy and not too large momentum transfers we found that this model taking into account the spin is available to describe not only the differential, total cross section and ρ, but also the existing experimental data on polarization. It allows to make some predictions about spin effects at high energies.

1 Introduction

The polarization data available at present for proton-proton scattering at relatively high energies are compatible with the s-channel helicity conservation [1–3] and show that the polarization contribution decreases with increasing energy as it is expected in terms of Regge pole exchanges. The data are insufficiently precise to provide unambiguous conclusion at the higher energy, although a contribution from the helicity-flip amplitude cannot be excluded [2,4–7]. The existing polarized experiments [8–11] at energy lower than LHC allow one to study spin properties of proton-pomeron vertex at intermediate energies while conclusions about spin properties of amplitudes at high t are derived as rule from model extrapolations. The main conclusion was made that pomeron exchange is expected to produce the observed small spin effects.

Proton (anti)proton scattering provides a unique opportunity to investigate the crossing-odd contribution and its properties, including the possibility of spin flip. Attempts to study spin effects for the standard pomeron and odderon (simple poles of partial amplitudes in the plane of the complex angular momentum j) were made not often, because of the lack of sufficiently accurate data on polarization at high energies. Only the data at energies FNAL [8–10] and relatively recent data from RHIC [11] (albeit at very small t, in the region of Coulomb-nuclear interference) are available. We would like to emphasize here that we do not consider in the given paper the CNI region, postponing this important subject for a further separate investigation.

Despite a long time interest to spin effects physics in hadron interaction the available data set is not rich in a soft kinematic region at high energies. Firstly, the main part of experiments was performed for meson-nucleon and electron-proton interactions. Secondly, these measurements were made at low and intermediate energies. Nevertheless, the available data stimulate permanently the theoretical and phenomenological studies of spin phenomena in a soft and hard kinematic, where different approaches (nonperturbative approaches from early [12] to relatively later and recent [6,7,13–17], and perturbative QCD) are exploring [18].

Interest in the role of the odderon in spin phenomena has recently increased markedly, which is partly due to recent data from TOTEM experiments [19–29]. Theoretical research, relatively speaking, is conducted in two directions. The first one is devoted mainly to odderon effects in elastic scattering, where pomeron and odderon are reggeons with the corresponding quantum numbers [16,17,30]. In the second direction, inelastic processes are studied [31,32], in which it is possible to detect pomeron and odderon as glueball resonances.

[a] e-mail: bencenorbert007@gmail.com
[b] e-mail: alexanderlengyel39@gmail.com
[c] e-mail: tarics1@rambler.ru
[d] e-mail: martynov@bitp.kiev.ua (corresponding author)
[e] e-mail: tersimonov@bitp.kiev.ua

Published online: 04 September 2021

As a rule, these studies are based on the perturbative results of QCD for pomeron (intercept $\alpha_{pom}(0) > 1$) and odderon (with $\alpha_{odd}(0) \leq 1$ [33,34]) and/or on the assumptions that they are simple reggeon j-poles.

Therefore, the idea naturally arises to apply the Froissaron and Maximal Odderon model to take into account the spin effects associated with Froissaron and Maximal Odderon (which are Regge singularities more complex than simple poles), for example, polarization data for pp, $\bar{p}p$ scattering at relatively high energies.

In this paper, we focus on elastic pp and $\bar{p}p$ scattering in the kinematic region

$$\begin{array}{llllll} \text{for} & \sigma_{tot}(s),\, \rho(s) & \text{at} & 5 \;\text{GeV} & \leq \sqrt{s} \leq 13 & \text{TeV}, \\ \text{for} & d\sigma(s,t)/dt & \text{at} & 19 \;\text{GeV} & \leq \sqrt{s} \leq 13 & \text{TeV} \\ \text{and} & & \text{at} & 0.05\;\text{GeV}^2 & \leq |t| \leq 14.2 & \text{GeV}^2. \end{array} \quad (1)$$

The main interest of the present paper is concentrated, after new measurements at the LHC, on the questions "Do Froissaron and Maximal Odderon flip spin?" and "How big are crossing-even and crossing-odd spin-flip amplitudes comparing with the corresponding spin-non-flip amplitudes?". We examine the issue in the framework of the FMO model.

To avoid the inevitable increase in the number of parameters, we use similarly to many authors [1–7,13–15] the simplified assumptions about the spin-non-flip and spin-flip amplitudes and their relationship.

The paper is organized as follows. In the next section the main formulas and general discussion of the problems are presented. In the Sect. 3.1 we describe the Simplified FMO amplitudes. In the Sect. 3.2 we discuss the original FMO model with spin-flip amplitudes. The results of comparison of both models with the data in region (1) are given in the Sect. 4.

2 Definitions and the FMO approach

2.1 Helicity amplitudes, observables

Generally the proton-proton and antiproton-proton scattering amplitude reads as

$$A^{pp}_{\bar{p}p}(s,t) = A^{(+)}(s,t) \pm A^{(-)}(s,t). \quad (2)$$

In this model we used the following normalization of the spin-averaged physical amplitudes

$$\begin{aligned} \sigma_t(s) &= \frac{1}{\sqrt{s(s-4m^2)}} \mathrm{Im} A(s,0), \\ \frac{d\sigma_{el}}{dt} &= \frac{1}{64\pi k s(s-4m^2)} |A(s,t)|^2 \end{aligned} \quad (3)$$

where $k = 0.3893797$ mb $\cdot$ GeV^2. With this normalization the amplitudes have dimension mb $\cdot$ GeV^2 and all the couplings are given in millibarns.

Taking into account the spin degrees of freedom in nucleon-nucleon elastic scattering still as a not well defined and quite complicated procedure. There are no strict and consequent methods in S-matrix theory to construct five independent helicity amplitudes for elastic nucleon-nucleon interaction, In this case, as in the spinless case, an important role are played by general physical arguments and by experimental data. Only various phenomenological models for these amplitudes have been constructed and analyzed.

We use the following definition of the helicity amplitudes.

$$\begin{aligned} \Phi_1(s,t) &= \langle ++|\mathcal{T}|++\rangle, \\ \Phi_2(s,t) &= \langle ++|\mathcal{T}|--\rangle, \\ \Phi_3(s,t) &= \langle +-|\mathcal{T}|+-\rangle, \\ \Phi_4(s,t) &= \langle +-|\mathcal{T}|-+\rangle, \\ \Phi_5(s,t) &= \langle ++|\mathcal{T}|+-\rangle. \end{aligned} \quad (4)$$

For the spin-averaged initial protons (antiprotons) the following equations for the total and differential cross sections and polarization are used

$$\sigma_{tot} = \frac{1}{\sqrt{s(s-4m^2)}} \mathrm{Im}\,(\Phi_1 + \Phi_3)\,, \quad (5)$$

$$\frac{d\sigma_{el}}{dt} = \frac{1}{16\pi k s(s-4m^2)} \times \left(|\Phi_1|^2 + |\Phi_2|^2 + |\Phi_3|^2 + |\Phi_4|^2 + 4|\Phi_5|^2\right), \quad (6)$$

$$P(t) = -2\frac{\mathrm{Im}[(\Phi_1 + \Phi_2 + \Phi_3 - \Phi_4)\Phi_5^*]}{|\Phi_1|^2 + |\Phi_2|^2 + |\Phi_3|^2 + |\Phi_4|^2 + 4|\Phi_5|^2}. \quad (7)$$

Each of these amplitudes has crossing-even and crossing-odd components $\Phi_i(s,t)$, $\quad i = 1, 2, ..., 5$

$$\Phi^{pp}_{\bar{p}p}(s,t) = \Phi^{(+)}(s,t) \pm \Phi^{(-)}(s,t). \quad (8)$$

Here, avoiding extra number of free parameters we, assume that $|\Phi_3| \ll |\Phi_1|, |\Phi_2|, |\Phi_4| \ll |\Phi_5|$ in accordance with an approximate factorization for Regge-terms and a common opinion that these spin amplitudes are small at high energies [1,2,4,6,7,13–15]. Moreover, we consider the oversimplified case: $\Phi_2 = \Phi_3 = \Phi_4 = 0$.

2.2 FMO approach

Let's comment shortly the Froissaron and Maximal Odderon approach to proton-(anti)proton elastic scattering. Two realizations of it are explored in the paper.

Historically it was formulated in [35] and applied [36–38] in description of high energy data on pp and $\bar{p}p$ scattering including the newest TOTEM data at 13 TeV.

The FMO model is built in the framework of the Regge approach taking into account the rigorous results and restrictions obtained in the theory of the analytic S-matrix. These results follow from the unitarity and analyticity of the interaction amplitudes.

A large number of parameters 36 in the model Ref. [38] is caused not by a wish to obtain at any cost the best description of the experimental data in the considered range of energies and momentum transfers (1). All terms of the FMO amplitude are important in various kinematic sub-regions. The secondary reggeons, f and ω determine properties of the model at relatively low energies, standard pomeron and odderon play role for the position and form of the dips and bumps in the differential cross sections, and all three terms in Froissaron and in Maximal Odderon are essential not only at the highest LHC energies. We would like to note here that the cancellation of the third terms in Froissaron and Maximal Odderon lead to a higher χ^2 (by more than 10 ‰), however, they are negligible at asymptotic energy. The model describes total number of experimental points 2386, with $\chi^2/NDF \approx 1.6$, where NDF = 2345 (the number of experimental points minus the number of parameters). Thus, on the average, we have more than 50 experimental points per one free parameter. We would like to emphasize well known fact that the kinematic region (1) is not suitable for perturbative QCD. It is known that only Regge-type models can more or less successfully describe the experimental data in this area. However, many numbers of unknown parameters is an attribute of Regge approach.

The maximal growth of the even-under-crossing amplitude $A^{(+)}$ allowed by unitarity:

$$A^{(+)}(s, t = 0) \propto is \ln^2 \tilde{s}, \quad \tilde{s} = -is/s_0, \quad s_0 = 1 \text{ GeV}^2 \tag{9}$$

lead to

$$\sigma \propto \ln^2(s/s_0). \tag{10}$$

The corresponding maximal behavior of the odd-under-crossing amplitude $A^{(-)}$

$$A^{(-)}(s, t = 0) \propto s \ln^2 \tilde{s} \tag{11}$$

leads via the optical theorem to the difference of the antiparticle-particle and particle-particle total cross sections

$$\Delta\sigma \propto \ln(s/s_0) \tag{12}$$

which grows, in absolute value, with energy. However, the sign of $\Delta\sigma$ is not fixed by general principles.

Such a behavior (10) is often referred to as "Froissaron", while the behavior (11) is termed as "Maximal Odderon". At $t = 0$, they correspond in the j-plane to a triple poles located at $j = 1$. Wherein Froissaron term is mainly imaginary while the Maximal Odderon one is mainly real term. It was shown in [36] that Froissaron and Maximal Odderon model describes well all the forward scattering TOTEM data [23–29], including the surprisingly small value of the ratio ρ at $\sqrt{s} = 13$ TeV. Moreover, fit to the data at $t = 0$ of the model with a more general form of FMO [37] shows that parameters return to the solution with Froissaron and Maximal Odderon.

The FMO model for the forward scattering [36,37] is still the only model that accurately describes and explains the results of the most recent measurements performed by TOTEM collaboration for zero momentum transfer, $t = 0$.

Extension of the FMO model for $t \neq 0$ was suggested in [38]. It leads to a qualitative agreement with the data in the region (1). The FMO model allowed to make certain conclusions about crossing-odd, odderon effects, which are confirmed by experimental data.

The interesting quark-diquark model is applied in [41] to describe and analyze the pp and $p\bar{p}p$ data at $\sqrt{s} > 0.5$ Tev. However, a behavior of the model at lower energies is not considered.

In the recent papers, [39] and the TOTEM and D0 collaborations [40], model-independent analysis of the data and the Odderon hypothesis was performed and the conclusive evidences of Odderon experimental discover are given. It has been noted in [40] "A reduction of the significance of a difference between pp and $\bar{p}p$ cross sections would only occur if the pp total cross section were larger than the $\bar{p}p$ total cross section at 1.96 TeV. This is the case only in maximal odderon scenarios [38]".

Thus, it would be interesting to consider at least some of the spin effects within this approach.

For a comparison we consider here the simplified version of the FMO model, which has less number of free parameters because pre-asymptotic terms in the Froissaron and Maximal Odderon are replaced by double pole pomeron and odderon contributions. The "hard" pomeron and odderon contributions are canceled as well. More details about these models are given in the Sects. 3.1, A and 3.2, B

3 The models for spin-non-flip and spin-flip amplitudes

As noted above, our aim is to study the spin-flip effects, assuming that they are determined mainly by the Φ_5 term. Therefore, we apply here the assumption $\Phi_2 = \Phi_3 = \Phi_4 = 0$ to the models considered. If $\Phi_3 \neq 0$ but has the same functional form as Φ_1, then just redefinition of the couplings in Φ_1 can be applied.

3.1 Simplified FMO model (Model A)

Only the main terms of Froissaron and Maximal Odderon amplitudes in FMO model [38] are taken into account in the model A. At $t = 0$ they correspond to triple poles in the j-plane. This truncated crossing-even and crossing-odd terms of FMO model are noted as $P_i^{(T)}(s, t)$ and $O_i^{(T)}(s, t)$, respectively.

Thus, in the model A the crossing-even and crossing-odd parts of the both spin amplitudes important at high energy are chosen as follows

$$\begin{aligned}\Phi_i^{(\pm)}(s,t) &= P_i(s,t) + R_i^f(s,t) \pm [O_i(s,t) + R_i^\omega(s,t)],\\ P_i(s,t) &= P_i^{(T)}(s,t) + P_i^{(D)}(s,t) + P_i^{(S)}(s,t),\\ O_i(s,t) &= O_i^{(T)}(s,t) + O_i^{(D)}(s,t) + O_i^{(S)}(s,t),\end{aligned} \tag{13}$$

where $i = 1, 5$. The full explicit expressions for the model A are given in A.

Spin-flip amplitudes are written in the model A in the following form

$$\begin{aligned}P_5^{(T,D,S,f)}(s,t) &= \frac{\sqrt{-t}}{2m}\lambda_+(t) P_1^{(T,D,S,f)}(s,t),\\ O_5^{(T,D,S,\omega)}(s,t) &= \frac{\sqrt{-t}}{2m}\lambda_-(t) O_1^{(T,D,S,\omega)}(s,t),\\ P_i^f &\equiv R_i^f, \quad O_i^\omega \equiv R_i^\omega.\end{aligned} \tag{14}$$

For $\lambda_\pm(t)$ we try three variants in the fit to experimental data:

$$\begin{aligned}&\text{V.1} \quad \lambda_\pm(t) = 1;\\ &\text{V.2} \quad \lambda_\pm(t) = 1 + p_\pm t;\\ &\text{V.3} \quad \lambda_\pm(t) = 1 + p_{1,\pm} t + p_{2,\pm} t^2.\end{aligned} \tag{15}$$

Matching the model with experimental data are given in Sect. 4.

3.2 Full FMO model (Model B)

For spin-non-flip amplitudes we use the FMO model at $t \neq 0$ [38]. The only difference with [38] is a notation for constants and functions.

$$\begin{aligned}\Phi_i^+(z_t,t) &= P_i^{(F)}(z_t,t) + P_i^{(1)}(z_t,t) + P_i^{(2)}(z_t,t)\\ &\quad + P_i^{(h)}(z_t,t) + R_i^+(z_t,t),\\ \Phi_i^-(z_t,t) &= O_i^{(M)}(z_t,t) + O_i^{(1)}(z_t,t) + O_i^{(2)}(z_t,t)\\ &\quad + O_i^{(h)}(z_t,t) + R_i^-(z_t,t).\end{aligned} \tag{16}$$

where $z_t = -1 + 2s/(4m^2 - t) \approx 2s/(4m^2 - t)$ and $i = 1, 5$.

In Eq. (16) $P_i^{(F)}$, $O_i^{(M)}$ are the Froissaron and Maximal Odderon contributions, $P_i^{(1)}$, $O_i^{(1)}$ are the standard (single j-pole) pomeron and odderon contributions and R_i^+, R_i^- are effective f and ω single j-pole contributions, where j is an angular momentum of these reggeons. $P_i^{(2)}$ and $O_i^{(2)}$ are double PP, OO and PO cuts, respectively. We take into account the "hard" pomeron and odderon $P_i^{(h)}$, $O_i^{(h)}$ as well.

We consider the model at $t \neq 0$ and at energy $\sqrt{s} > 19$ GeV, so we neglect the rescattering of secondary reggeons R_1^+, R_1^- with P and O. In the considered kinematic region they are small. Besides, because f and ω are effective, they can take into account small effects from the cuts via their parameters.

The explicit expressions for the spin-non-flip amplitudes in the full FMO model are given in Sect. B.

We used the following forms of spin-flip amplitudes for the fit:

$$\begin{aligned}\Phi_5^+(z_t,t) &= \frac{\sqrt{-t}}{2m}\lambda_+(t)\\ &\quad \times \left\{P_5^{(F)}(z_t,t) + P_5^{(eff)}(z_t,t) + R_5^+(z_t,t)\right\},\\ \Phi_5^-(z_t,t) &= \frac{\sqrt{-t}}{2m}\lambda_-(t)\\ &\quad \times \left\{O_5^{(M)}(z_t,t) + O_5^{(eff)}(z_t,t) + R_5^-(z_t,t)\right\}.\end{aligned} \tag{17}$$

For the sake of reduced number of free parameters we consider the sum of all standard pomeron (odderon) terms as one effective pomeron (odderon):

$$\begin{aligned}P_1^{(eff)}(z_t,t) &= P_1^{(1)}(z_t,t) + P_1^{(2)}(z_t,t) + P_1^{(h)}(z_t,t),\\ O_1^{(eff)}(z_t,t) &= O_1^{(1)}(z_t,t) + O_1^{(2)}(z_t,t) + O_1^{(h)}(z_t,t).\end{aligned} \tag{18}$$

Then

$$\begin{aligned}P_5^{(F)}(z_t,t) &= h_5 e^{\beta_5(F)\tau_p} P_1^{(F)}(z_t,t),\\ \tau_p &= 2m_\pi - \sqrt{4m_\pi^2 - t},\\ P_5^{(eff)}(z_t,t) &= g_5^{(P)} e^{\beta_5(P)\tau_p} P_1^{(eff)}(z_t,t),\\ R_5^+(z_t,t) &= g_{5,+} e^{\beta_5^+\tau_p} R_1^+(z_t,t),\end{aligned} \tag{19}$$

$$\begin{aligned}O_5^{(M)}(z_t,t) &= o_5 e^{\beta_5(M)\tau_o} O_1^{(M)}(z_t,t),\\ \tau_0 &= 3m_\pi - \sqrt{9m_\pi^2 - t},\\ O_5^{(eff)}(z_t,t) &= g_5^{(O)} e^{\beta_5(O)\tau_o} O_1^{(eff)}(z_t,t),\\ R_5^-(z_t,t) &= g_{5,-} e^{\beta_5^-\tau_o} R_1^-(z_t,t).\end{aligned} \tag{20}$$

For the functions $\lambda_+ \pm(t)$ we have explored the same variants as used in the model A (Sect. 3.1).

4 Results

Free parameters of the models were determined from the fit to the data on $\sigma_{tot}(s)$, $\rho(s,0)$, $d\sigma(s,t)/dt$ and $P(t)$ in the region (1).

The data on σ_{tot} and ρ are taken from the Particle Data Group site [43]. The recent TOTEM data [19–29] also were added. We did not include to the fit two ATLAS points on σ_{tot} at 7 and 8 TeV (see discussion in [37]). The data on differential cross sections were collected from the big number ot the papers from FNAL, ISR, CERN and other experimental collaborations. They can be found at the Repository for publication-related High-Energy Physics data [44]. Data on polarization included in the data set for fit are taken from Refs. [9,10]. In the data set there are only published data (copied either from the journal versions or from the Durham HEP Data). The errors (systematical and statistical ones often are not shown in the old papers) were added in quadrature

Table 1 Data description in the Simplified FMO model (S-FMO) and original FMO model (FMO) with the three choices of the functions $\lambda_{\pm}(t)$ in the spin-fip amplitudes. N is the total number of experimental points in the fit. Comments on the number of free parameters in fits are given in the main text of the Sect. 4

Process	Observable	N_o	S-FMO model, χ^2/NDF Variants of $\lambda_{\pm}(t)$ in Eqs. (14), (15)			FMO model, χ^2/NDF		
			V1	V2	V3	V1	V2	V3
$pp \to pp$	σ_{tot}	110	0.899	0.864	0.865	0.861	0.857	0.849
$\bar{p}p \to \bar{p}p$	σ_{tot}	58	2.193	1.271	1.130	0.812	0.821	0.823
$pp \to pp$	ρ	67	1.788	1.586	1.587	1.594	1.587	1.599
$\bar{p}p \to \bar{p}p$	ρ	12	1.267	0.658	0.595	0.498	0.551	0.576
$pp \to pp$	$d\sigma/dt$	1701	1.728	1.630	1.587	1.531	1.512	1.501
$\bar{p}p \to \bar{p}p$	$d\sigma/dt$	389	1.359	0.943	0.919	0.930	0.986	0.933
$pp \to pp$	$P(t)$	49	0.920	1.742	1.483	0.833	0.1053	1.053
	n_{par}, number of free parameters		35	37	38	41	43	45
	$\chi^2/NDF = \chi^2/(\sum_p N_p - n_{par})$		1.648	1.493	1.449	1.391	1.392	1.377

if they were shown separately without normalization uncertainties.

Results of the fits in all considered variants of the models A and B are shown in Table 1. Because of the relatively small differences in χ^2 we show the Figs. 1, 2, 4 and 5 with theoretical curves for both the models in the simplest variants V1 with $\lambda_{\pm} = 1$. The values and errors of free parameters in the chosen variant V1 are given in Table 2. The number of free parameters is varied in various fits, because we put a reasonable (in our opinion) limits for slopes in the exponential vertexes ($0 \le b(\beta) \le 20\ \mathrm{GeV}^{-2(1)}$) and for those of trajectories ($0.8 \le \alpha'_{f,\omega} \le 1.1\ \mathrm{GeV}^{-2}$). If during the fiting such a parameter goes to the limit value, then it is fixed at the corresponding limit.

We would like to note here a little bit overestimated total cross sections at the highest energies and as consequence lower absolute values of the ratio ρ in the Simplified FMO model. Additional terms, the "hard" pomeron and odderon (exactly as it is written in the original FMO model) can fix the problem (then χ^2 and curves for σ_{tot}, ρ in both the models almost coincide). We do not discuss here this solution.

One can see from the Figures that both the considered models do not contradict the data on differential cross sections and polarization in the kinematic region (1).

In the Figs. 2, 3 and 4 we added for a comparison the curves (red dot lines) calculated without spin-flip amplitudes. One can see that at $|t| < 2\,\mathrm{GeV}^2$ differences of the differential cross sections are small. They are varied from 1 to ~10 percents, at some energies only at points close to dip they increase to values $\lesssim$ 20–30%. However, at higher $|t|$ the differences are higher. We wold like to note that this t-region is out of available data on polarization. This phenomenon requires further analysis when new data at more high energies and t will be known. The same is concerning the ratios shown in the Figs. 6 and 7.

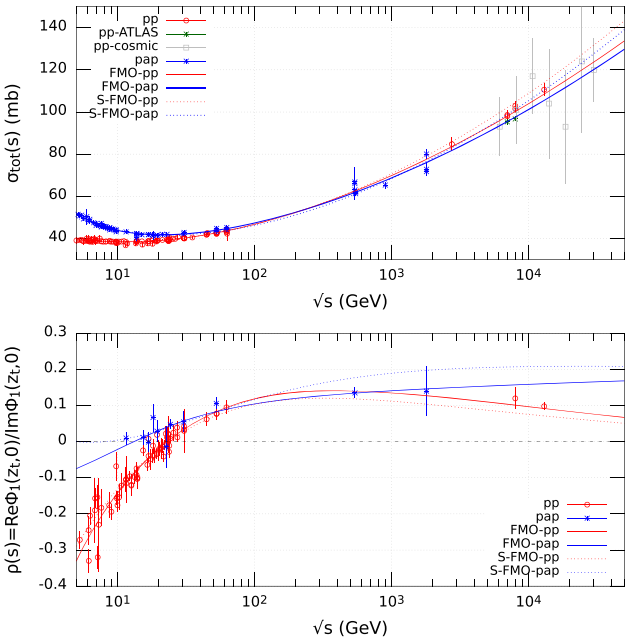

Fig. 1 Total cross sections σ_{tot} and ratio ρ in the variant V1 for models A (dotted line) and B (solid line), $z_t(t=0) = s/2m^2 - 1$

Figure 6 demonstrates that the ratios of spin-flip amplitudes to spin-non-flip ones are more important in FMO model then in S-FMO almost at any considered $|t|$.

One can see in Fig. 7 the influence of odderon in the spin-non-flip and spin-flip amplitudes in the considered models. Contribution of the Maximal Odderon in non-flip amplitudes at not highest energies is stronger in the original FMO model (red lines) and does not decrease with $|t|$ as in the S-FMO model (blue lines). In the "TeV" region situation only the relative decreasing of S-FMO model is observed. The Maximal Odderon to Froissaron terms ratio in the spin-flip components (dashed lines) ($|\Phi_5^-|/|\Phi_5^+| \approx 10\%$ at the $|t| \gtrsim 1-2\ \mathrm{GeV}^2$)

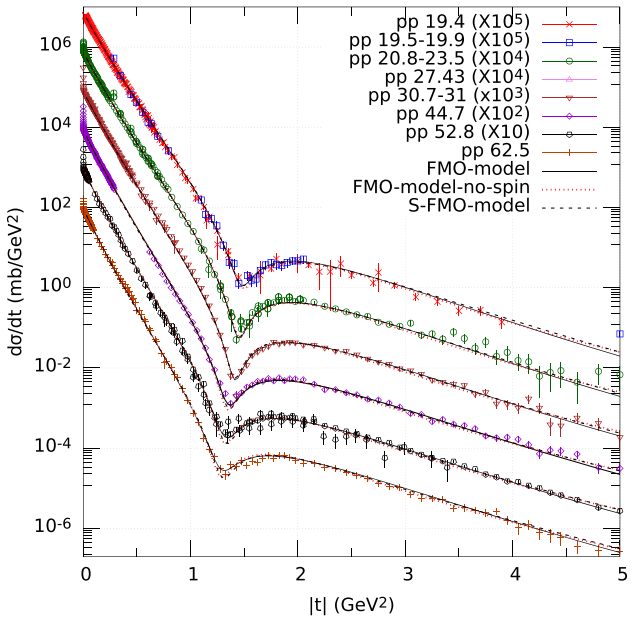

Fig. 2 Differential $pp \to pp$ cross sections at the FNAL and ISR energies

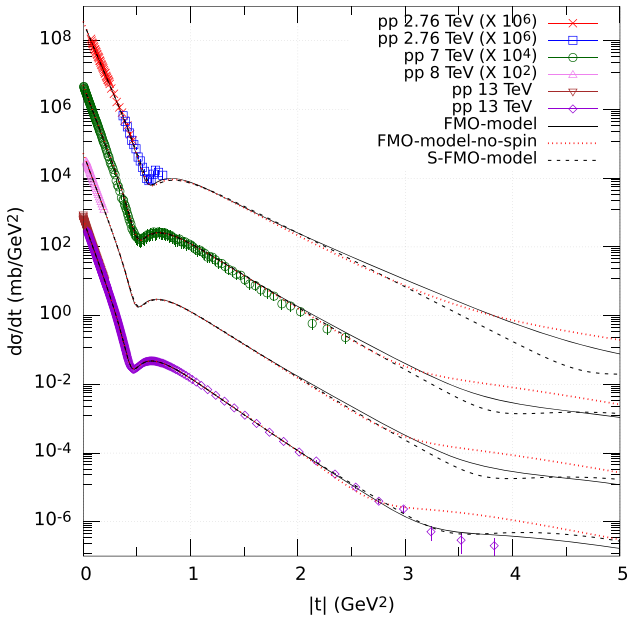

Fig. 3 Differential $pp \to pp$ cross sections at the LHC energies

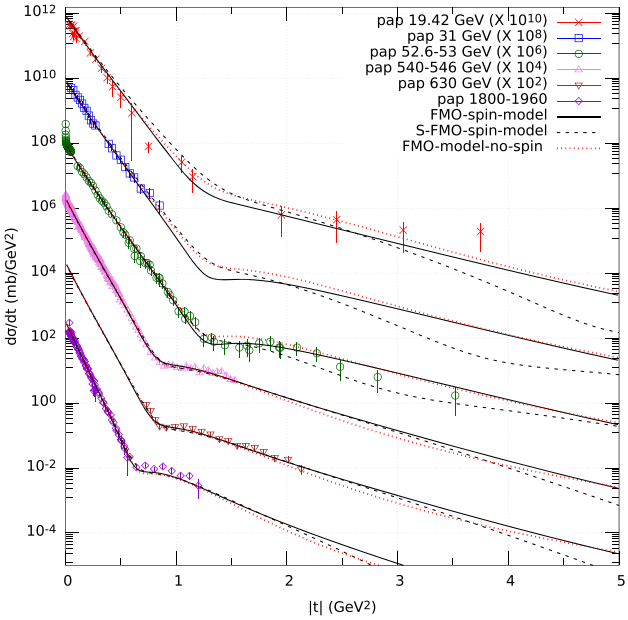

Fig. 4 Differential $\bar{p}p \to \bar{p}p$ cross sections at the FNAL, ISR, SPS and Tevatron energies

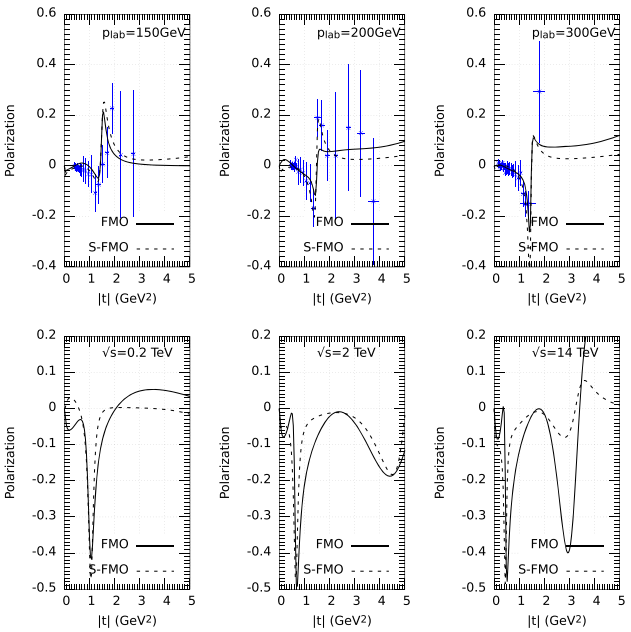

Fig. 5 Polarization at the FNAL energies, and extrapolation of $P(t)$ up to $\sqrt{s} = 13$ TeV. Data at $p_{lab} = 150$ GeV did not included in the fit

in these models is obviously higher than it was estimated in [2] (∼2%).

These observations in fact give the answers to the questions addressed in the Introduction about the role and magnitude of spin effects in the models within the FMO approach. Evidently, Froissaron and Maximal Odderon flip the nucleon spin, contribution of the crossing-even and crossing-odd amplitude to observable quantities is higher than in the models with traditional pomeron and odderon. The last estimation requires a verification when the new data will be available at higher energies.

We confirm conclusions of Refs. [1,2,4,6,7,14] obtained in more traditional pomeron and odderon models that the crossing-even and crossing-odd spin-flip amplitudes are important for agreement with experimental data. It would be not worse to note that polarization in the S-FMO model

Table 2 Parameters of the Simplified FMO model (A) and full model (B)

Model A				Model B			
Name	Dimension	Value	Error	Name	Dimension	Value	Error
$g_{1,p}^{(T)}$	mb	0.29343E+00	0.22854E–03	$h_{1,1}$	mb	0.22978E+00	0.18848E–03
$\beta_{1,p}^{(T)}$	GeV^{-1}	0.51823E+01	0.25651E–02	$h_{1,2}$	mb	0.11223E+00	0.20510E–02
r_p		0.29661E+00	0.57101E-04	$h_{1,3}$	mb	0.14071E+02	0.71014E–01
α'_p	GeV^{-2}	0.16361E+00	0.39431E–03	r_+		0.31165E+00	0.52057E–04
$g_{1,p}^{(D)}$	mb	−0.76106E+00	0.11876E–02	$\beta_{1,1}^{(F)}$	GeV^{-1}	0.31822E+01	0.17910E–02
$\beta_{1,p}^{(D)}$	GeV^{-1}	0.19434E+01	0.32444E-02	$\beta_{1,2}^{(F)}$	GeV^{-1}	0.16873E+01	0.14904E–01
$g_{1,p}^{(S)}$	mb	0.27402E+02	0.40164E–01	$\beta_{1,3}^{(F)}$	GeV^{-1}	0.59988E+01	0.36649E–01
$\beta_{1,p}^{(S)}$	GeV^{-1}	0.41323E+01	0.38042E–02	$o_{1,1}$	mb	−0.57797E–01	0.88763E–04
$g_{1,o}^{(T)}$	mb	−0.37472E-01	0.22257E-03	$o_{1,2}$	mb	0.12060E+01	0.14749E–01
$\beta_{1,o}^{(T)}$	GeV^{-1}	0.33673E+01	0.93166E–02	$o_{1,3}$	mb	−0.15041E+02	0.62755E–01
r_o		0.27253E+00	0.24894E–03	r_-		0.60104E-01	0.82785E–04
α'_o	GeV^{-2}	0.12120E-01	0.45999E–03	$\beta_{1,1}^{(O)}$	GeV^{-1}	0.17748E+01	0.20315E–02
$g_{1,o}^{(D)}$	mb	0.20536E+00	0.25831E-02	$\beta_{1,2}^{(O)}$	GeV^{-1}	0.15147E+02	0.52950E+00
$\beta_{1,o}^{(D)}$	GeV^{-1}	0.65245E+01	0.35911E-01	$\beta_{1,3}^{(O)}$	GeV^{-1}	0.28054E+01	0.44815E–02
$g_{1,o}^{(S)}$	mb	0.13783E+01	0.14165E-01	α'_p	GeV^{-2}	0.14729E+00	0.26247E–03
$\beta_{1,o}^{(S)}$	GeV^{-1}	0.34116E+01	0.12406E–01	$g_1^{(P)}$	mb	0.30616E+02	0.40503E–01
$\alpha_f(0)$		0.76576E+00	0.15048E–02	d_p	mb	0.78722E+00	0.11601E–02
α'_f	GeV^{-2}	0.80000E+00	Fix at lim	$b_{1,1}^{(P)}$	GeV^{-2}	0.53807E+01	0.72308E–02
$g_1^{(f)}$	mb	0.35167E+02	0.24485E+00	$b_{1,2}^{(P)}$	GeV^{-2}	0.21605E+01	0.59669E–02
$\beta_1^{(f)}$	GeV^{-1}	0.00000E+00	Fix at lim	α'_o	GeV^{-2}	0.20000E–02	0.12652E–02
$\alpha_\omega(0)$		0.61636E+00	0.58521E-02	$g_1^{(Od)}$	mb	0.16736E+02	0.23224E–01
α'_ω	GeV^{-2}	0.80000E+00	Fix at lim	d_o	mb	0.87167E+00	0.55703E–03
$g_1^{(\omega)}$	mb	0.24366E+02	0.35434E+00	$b_{1,1}^{(Od)}$	GeV^{-2}	0.61792E+01	0.67464E–02
$\beta_1^{(\omega)}$	GeV^{-1}	0.20000E+02	fix at lim	$b_{1,2}^{(Od)}$	GeV^{-2}	0.20719E+01	0.38476E–02
$g_{5,p}^{(T)}$	mb	0.98237E+00	0.29269E–02	$\alpha_f(0)$		0.65048E+00	0.19140E–02
$\beta_{5,p}^{(T)}$	GeV^{-1}	0.97449E+01	0.11045E–01	α'_f	GeV^{-2}	0.80000E+00	Fix at lim
$g_{5,p}^{(D)}$	mb	−0.23787E+02	0.71732E-01	$g_1^{(f)}$	mb	0.50043E+02	0.38370E+00
$\beta_{5,p}^{(D)}$	GeV^{-1}	0.12183E+02	0.11698E–01	$b_{1,f}$	GeV^{-2}	0.00000E+00	0.00000E+00
$g_{5,p}^{(S)}$	mb	0.29036E+03	0.70315E+00	$\alpha_\omega(0)$		0.22000E+00	0.99194E–02
$\beta_{5,p}^{(S)}$	GeV^{-1}	0.97486E+01	0.80005E–02	α'_ω	GeV^{-1}	0.11000E+01	fix at lim
$g_{5,o}^{(T)}$	mb	0.57721E-03	0.57266E-03	$g_1^{(\omega)}$	mb	0.38668E+02	0.69599E+00
$\beta_{5,o}^{(T)}$	GeV^{-1}	0.26306E+01	0.96362E+00	$b_{1,\omega}$	GeV^{-2}	0.00000E+00	0.00000E+00
$g_{5,o}^{(D)}$	mb	0.77319E+01	0.13988E+00	$g_{p,h}$	mb	−0.15778E+02	0.24747E–01
$\beta_{5,o}^{(D)}$	GeV^{-1}	0.14185E+02	0.63904E–01	$t_{p,h}$	GeV^2	0.49795E+00	0.51099E–03
$g_{5,o}^{(S)}$	mb	−0.69382E+02	0.14333E+01	$g_{o,h}$	mb	0.23187E+02	0.29454E-01
$\beta_{5,o}^{(S)}$	GeV^{-1}	0.12588E+02	0.79085E–01	$t_{o,h}$	GeV^2	0.57226E+00	0.45421E–03
$g_5^{(f)}$	mb	−0.58675E+03	0.12276E+02	h_5	mb	0.38469E+01	0.56953E–02

Table 2 continued

Model A				Model B			
Name	Dimension	Value	Error	Name	Dimension	Value	Error
$\beta_5^{(f)}$	GeV^{-1}	0.92251E+01	0.12837E+00	$\beta_5^{(F)}$	GeV^{-1}	0.14698E+01	0.57266E–02
$g_5^{(\omega)}$	mb	0.29637E+02	0.17742E+01	o_5	mb	0.19514E+01	0.85428E–02
$\beta_5^{(\omega)}$	GeV^{-1}	0.00000E+00	Fix at lim	$\beta_5^{(O)}$	GeV^{-1}	0.18374E+01	0.12180E–01
				$g_{5,p}$	mb	0.17196E+01	0.10140E–01
				$\beta_{5,p}$	GeV^{-1}	0.10052E+01	0.16212E–01
				$g_{5,o}$	mb	0.44713E+00	0.46582E–02
				$\beta_{5,o}$	GeV^{-1}	0.00000E+00	Fix at limt
				$g_{5,f}$	mb	0.97840E+00	0.21964E–01
				$\beta_{5,f}$	GeV^{-1}	0.00000E+00	Fix at lim
				$g_{5,\omega}$	mb	0.18768E+02	0.81228E+00
				$\beta_{5,\omega}$	GeV^{-1}	0.00000E+00	0.00000E+00

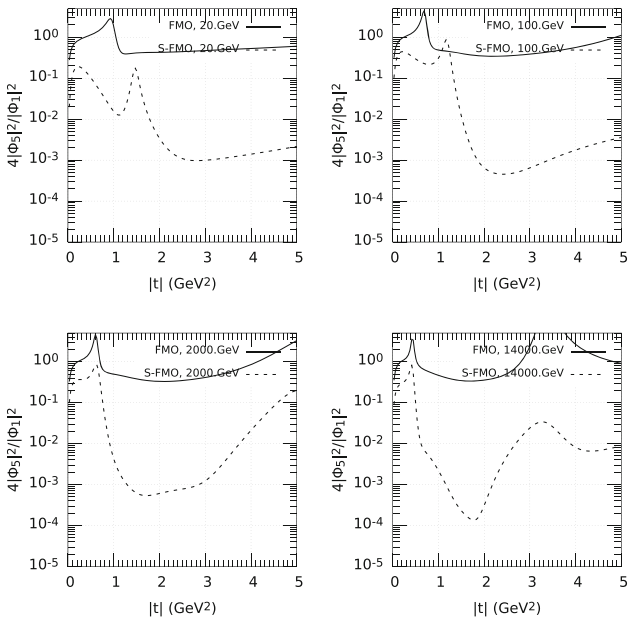

Fig. 6 Ratio $4|\Phi_5|^2/|\Phi_1|^2$ of the contributions to differential pp cross sections

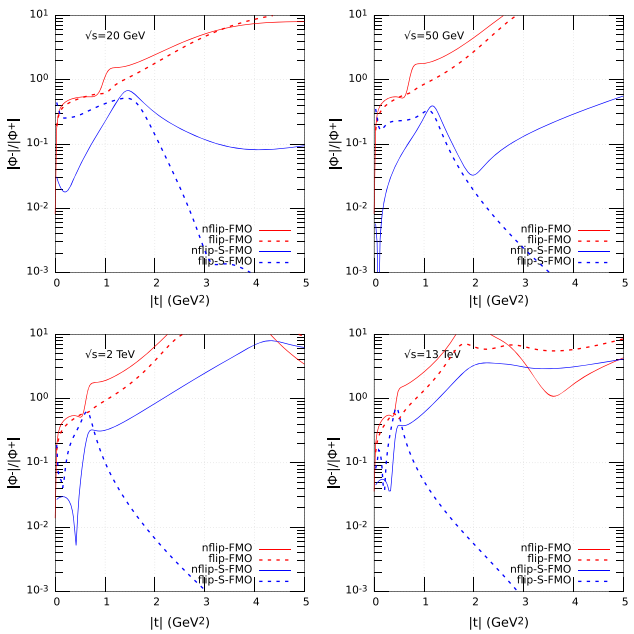

Fig. 7 The ratios of crossing-odd to crossing-even parts of the spin-non-flip (solid lines) and spin-flip (dashed lines) amplitudes in the FMO and S-FMO models

goes to 0 with rising $|t|$, while in the original FMO it does not vanish at least at a few GeV^2.

In conclusion, we would like to emphasize that considered FMO models taking into account the spin-flip effects are in a qualitative agreement with available experimental data. They predict more important role of the spin-flip amplitudes at higher energies and momenta transferred than it is predicted by the traditional Regge pole models. Unfortunately, however, there are no data at high energy to confirm or deny these predictions.

Acknowledgements We thank Prof. B. Nicolescu and Prof. S.M. Troshin for a careful reading the manuscript, comments and useful discussions. E.M. and G.T. were partially supported by the Project of the National Academy of Sciences of Ukraine (0118U003197).

Data Availability Statement This manuscript has no associated data or the data will not be deposited. [Author's comment: The datasets generated and used during the study are available in the HEPdata repository, https://www.hepdata.net. These datasets are available as well from the corresponding author on reasonable request.]

Appendix A: Simplified FMO model

The simple and dipole Pomerons (Odderons) for both components have a conventional form:

$$\begin{aligned} P_1^{(S)}(s,t) &= -g_{1,p}^{(S)}\tilde{s}^{\alpha_p(t)}e^{\beta_{1,p}^{(S)}\tau_p}, \\ P_1^{(D)}(s,t) &= -g_{1,p}^{(D)}\xi\tilde{s},^{\alpha_p(t)}\, e^{\beta_{1,p}^{(D)}\tau_p}, \\ \tau_p &= 2m_\pi^2 - \sqrt{4m_\pi^2 - t}, \end{aligned} \tag{A.1}$$

$$\begin{aligned} O_1^{(S)}(s,t) &= ig_{1o}^{(S)}\tilde{s}^{\alpha_o(t)}e^{\beta_{1,o}^{(S)}\tau_o}, \\ O_1^{(D)}(s,t) &= ig_{1,o}^{(D)}\xi\tilde{s}^{\alpha_o(t)}e^{\beta_{1,o}^{(D)}\tau_0}, \\ \tau_0 &= 3m_\pi^2 - \sqrt{9m_\pi^2 - t}. \end{aligned} \tag{A.2}$$

where $\tilde{s} = -i(s-2m^2)/2m^2$, $\xi = \ln(\tilde{s})$.

It is important that we use for single and double j-poles the pomeron and odderon intercepts equal to one

$$\alpha_p(t) = 1 + \alpha_p' t, \qquad \alpha_o(t) = 1 + \alpha_o' t. \tag{A.3}$$

avoiding a violation of unitary restriction for total cross sections.

$$\begin{aligned} P_5^{(S)}(s,t) &= -g_{5,p}^{(S)}\frac{\sqrt{-t}}{2m}\lambda_+(t)\tilde{s}^{\alpha_p(t)}e^{\beta_{5,p}^{(S)}\tau_p}, \\ P_5^{(D)}(s,t) &= -g_{5,p}^{(D)}\frac{\sqrt{-t}}{2m}\lambda_+(t)\xi\tilde{s}^{\alpha_p(t)}e^{\beta_{5,p}^{(D)}\tau_p}, \\ O_5^{(S)}(s,t) &= ig_{5,o}^{(S)}\frac{\sqrt{-t}}{2m}\lambda_-(t)\tilde{s}^{\alpha_o(t)}e^{\beta_{1,o}^{(S)}\tau_o}, \end{aligned} \tag{A.4}$$

$$O_5^{(D)}(s,t) = ig_{5,o}^{(D)}\frac{\sqrt{-t}}{2m}\lambda_-(t)\xi\tilde{s}^{\alpha_o(t)}e^{\beta_{5,0}^{(DS)}\tau_p o} \tag{A.5}$$

where m is proton mass. A choice of $\lambda_\pm(t)$ is discussed in the Sect. 3.1 .

The tripole terms $P^{(T)}$, $O^{(T)}$, containing only asymptotic main components from the Froissaron and Maximal Odderon [38]), which are defined in according with the AKM asymptotic theorem [42]

$$\begin{aligned} P_1^{(T)}(s,t) &= -g_{1,p}^{(T)}\tilde{s}\xi^2\frac{2J_1(z_p)}{z_p}e^{\beta_{1,p}^{(T)}\tau_p}, \\ P_5^{(T)}(s,t) &= -g_{5,p}^{(T)}\frac{\sqrt{-t}}{2m}\lambda_p(t)\tilde{s}\xi^2\frac{2J_1(z_p)}{z_p}e^{\beta_{5,p}^{(T)}\tau_p}, \\ O_1^{(T)}(s,t) &= ig_{1,o}^{(T)}\tilde{s}\xi^2\frac{2J_1(z_o)}{z_o}e^{\beta_{1,o}^{(T)}\tau_o}, \end{aligned} \tag{A.6}$$

$$O_5^{(T)}(s,t) = ig_{5,o}^{(T)}\frac{\sqrt{-t}}{2m}\lambda_o(t)\tilde{s}\xi^2\frac{2J_1(z_o)}{z_o}e^{\beta_{1,o}^{(T)}\tau_o}, \tag{A.7}$$

where $z_p = r_p\tau\xi$, $z_o = r_o\tau\xi$, $\tau = \sqrt{-t/t_0}$, $t_0 = 1\,\mathrm{GeV}^2$, r_p, r_o are constants.

Contributions of the secondary reggeons, f and ω have a standard form

$$\begin{aligned} R_1^{(f)}(s,t) &= -g_1^{(f)}\tilde{s}^{\alpha_f(t)}e^{\beta_1^{(f)}\tau_p}, \\ R_5^{(f)}(s,t) &= -g_5^{(f)}\frac{\sqrt{-t}}{2m}\lambda_p(t)\tilde{s}^{\alpha_f(t)}e^{\beta_5^{(f)}\tau_p}, \\ \alpha_f(t) &= \alpha_f(0) + \alpha_f' t, \end{aligned} \tag{A.8}$$

$$\begin{aligned} R_1^{(\omega)}(s,t) &= ig_1^{(\omega)}\tilde{s}^{\alpha_f(t)}e^{\beta_1^{(\omega)}\tau_o}, \\ R_5^{(\omega)}(s,t) &= ig_5^{(\omega)}\frac{\sqrt{-t}}{2m}\lambda_o(t)\tilde{s}^{\alpha_\omega(t)}e^{\beta_5^{(\omega)}\tau_o}, \\ \alpha_\omega(t) &= \alpha_\omega(0) + \alpha_\omega' t. \end{aligned} \tag{A.9}$$

Appendix B: Original FMO model

We write here the explicit spin-non-flip terms of the FMO model at $t \le 0$ [38] just for reader's convenience. The only difference of [38] is a notation for constants and functions. Spin-flip terms are presented and discussed in Sect. 3.2.

Froissaron and Maximal Odderon are written in the following form

$$\begin{aligned} \frac{1}{iz}P_1^{(F)}(z_t,t) &= h_{1,1}\xi^2\frac{2J_1(r_+\tau\xi)}{r_+\tau\xi}e^{\beta_{1,1}^{(F)}\tau_p} \\ &+ h_{1,2}\xi\frac{\sin(r_+\tau\xi)}{r_+\tau\xi}e^{\beta_{1,2}^{(F)}\tau_p} + h_{1,3}J_0(r_+\tau\xi)e^{\beta_{1,3}^{(F)}\tau_p}, \end{aligned} \tag{B.10}$$

$$\begin{aligned} \frac{1}{z}O_1^{(M)}(z_t,t) &= o_{1,1}\xi^2\frac{2J_1(r_-\tau\xi)}{r_-\tau\xi}e^{\beta_{1,1}^{(O)}\tau_o} \\ &+ o_{1,2}\xi\frac{\sin(r_-\tau\xi)}{r_-\tau\xi}e^{\beta_{1,2}^{(OM)}\tau_o} + o_{1,3}J_0(r_-\tau\xi)e^{\beta_{1,3}^{(M)}\tau_o}, \end{aligned} \tag{B.11}$$

where $z = 2m^2 z_t$, $\xi = \ln(-iz_t)$, $\tau = \sqrt{-t/t_0}$, $t_0 = 1\,\mathrm{GeV}^2$, $r_- = r_+ - \delta r_-$, $\delta r_- \ge 0$.

The effective secondary Regge pole contributions (crossing-even f and crossing-odd ω) have the form

$$\begin{aligned} R_1^{(K)}(z_t,t) &= -\binom{1}{i}2m^2 g_1^{(K)}(-iz_t)^{\alpha_K(t)}e^{b_1^{(K)}t} \\ \alpha_K(t) &= \alpha_K(0) + \alpha_K' t, \quad K = f, \omega \end{aligned} \tag{B.12}$$

In order to perform calculations of the standard pomeron and odderon cuts in explicit analytical form we have made replacement $z_t \to z_0 = z_t(t=0)$

$$\begin{aligned} R_1^{(L)}(z_0,t) &= -\binom{1}{i}2m^2 g_1^{(L)}(-iz_0)^{\alpha_L(t)} \\ &\times \left[d_L e^{b_{1,1}^{(L)}t} + (1-d_L)e^{b_{1,2}^{(L)}t}\right], \\ \alpha_L(t) &= 1 + \alpha_L' t, \quad L = P, O. \end{aligned} \tag{B.13}$$

This parametrization takes into account a possibility of a non pure exponential behavior of the vertex functions for the standard pomeron and odderon [38].

The factor $2m^2$ is inserted in amplitudes f, ω, P, O in order to have the normalization for amplitudes and dimension of coupling constants (in milliibarns) coinciding with those in [36].

We have added in the FMO the double pomeron and odderon cuts, PP, OO, PO in their usual standard form without any new parameters as well. Namely,

$$P_1^{(2)}(z_t,t) = P_1^{(PP)}(z_t,t) + P_1^{(OO)}(z_t,t),$$
$$O_1^{(2)}(z_t,t) = P_1^{(PO)}(z_t,t), \tag{B.14}$$

$$P_1^{(PP)}(z_t,t) = -i\frac{2m^2(z_0 g_1^{(P)})^2}{16\pi ks\sqrt{1-4m^2/s}}\left\{\frac{d_p^2}{2B_1^p}\exp(tB_1^p/2) + \frac{2d_p(1-d_p)}{B_1^p+B_2^p}\exp\left(t\frac{B_1^pB_2^p}{B_1^p+B_2^p}\right) + \frac{(1-d_p)^2}{2B_2^p}\exp(tB_2^p/2)\right\}, \tag{B.15}$$

$$P_1^{OO}(z_t,t) = -i\frac{2m^2(z_0 g_1^{(O)})^2}{16\pi ks\sqrt{1-4m^2/s}}\left\{\frac{d_o^2}{2B_1^o}\exp(tB_1^o/2) + \frac{2d_o(1-d_o)}{B_1^o+B_2^o}\exp\left(t\frac{B_1^oB_2^o}{B_1^o+B_2^o}\right) + \frac{(1-d_o)^2}{2B_2^o}\exp(tB_2^o/2)\right\}, \tag{B.16}$$

$$P_1^{PO}(z_t,t) = \frac{2m^2 z_t^2 g_1^{(P)} g_1^{(O)}}{16\pi ks\sqrt{1-4m^2/s}} \times \left\{\frac{d_p d_o}{B_1^p+B_1^o}\exp\left(t\frac{B_1^pB_1^o}{B_1^p+B_1^o}\right) + \frac{d_p(1-d_o)}{B_1^p+B_2^o}\exp\left(t\frac{B_1^pB_2^o}{B_1^p+B_2^o}\right) + \frac{(1-d_p)d_o}{B_2^p+B_1^o}\exp\left(t\frac{B_2^pB_1^o}{B_2^p+B_1^o}\right) + \frac{(1-d_p)(1-d_o)}{B_2^p+B_2^o}\exp\left(t\frac{B_2^pB_2^o}{B_2^p+B_2^o}\right)\right\} \tag{B.17}$$

where $B_k^{p,o} = b_{1,k}^{P,O} + \alpha'_{P,0}\ln(-iz_0)$, $k = 1,2$, $b_{1,k}^{P,O}$ are the constants from single pomeron and odderon contributions.

In [38] it was noted that for a better description of the data it is advisable to add to the amplitudes the contributions that mimic some properties of "hard" pomeron (P^h) and odderon (O^h). We take them in the simplest form

$$P_1^{(h)}(t) = i2m^2 z_t\frac{g_{h,p}}{(1-t/t_{p,h})^4},$$
$$O_1^{(h)}(t) = 2m^2 z_t\frac{g_{h,o}}{(1-t/t_{o,h})^4}. \tag{B.18}$$

References

1. N.H. Buttimore et al. The spin dependence of high-energy proton scattering. Phys. Rev. **D59**, 114010 (1999). arxiv:hep-ph/9901339v1
2. E. Leader, *Spin in Particle Physics* (Cambridge University Press, Cambridge, 2001), p. 500
3. C. Ewerz, P. Lebiedowicz, O. Nachtmann, A. Szczurek, Phys. Lett. B **763**, 382 (2016). arxiv:1606.08067v1
4. S. Donnachie, G. Dosch, P. Landshoff, O. Nachtmann, *Pomeron Physics and QCD* (Cambridge University Press, Cambridge, 2002)
5. S.M. Troshin, N.E. Tyurin, *Spin Phenomena in Particle Interactions* (World Scientific Publishing Company, Singapore, 1994), p. 224
6. A.F. Martini, E. Predazzi, Diffractive effects in spin flip pp amplitudes and predictions for relativistic energies. Phys. Rev. D **66**, 034029 (2002). arXiv:0209.027v1
7. K. Hinotani, H.A. Neal, E. Predazzi, G. Walters, Behavior of the spin-flip amplitude in high-energy proton-proton and pion-proton elastic scatterings. Nuovo Cimento **52A**, 363 (1979)
8. G. Fidecaro et al., Measurement of the polarization parameter in pp elastic scattering at p_{lab}=150 GeV/c. Nucl. Phys. **B173**, 513 (1980)
9. G. Fidecaro et al., Measurement of the differential cross section and of the polarization parameter in pp elastic scattering at p_{lab}=200 GeV/c. Phys. Lett. **105B**, 309 (1981)
10. R.V. Kline et al., Polarization parameters and angular distributions in pi-p elastic scattering at 100 GeV/c and in pp elastic scattering at p_{lab}100 GeV/c and 300 GeV/c. Phys. Rev. D **22**, 553 (1980)
11. L. Adamczyk et al., STAR Collaboration, Single spin asymmetry A_N in polarized proton–proton elastic scattering at $\sqrt{s}$= 200 GeV, Phys. Lett. B **719**, 62–69 (2013). arxiv:1206.1928v3
12. K.G. Boreskov, A.M. Lapidus, S.T. Sukhorukov, K.A. Ter-Martirosyan, Elastic scattering and charge exchange reactions at high energy in the theory of complex angular momentum. Sov. J. Nucl. Phys. **14**, 814 (1971)
13. J.-R. Cudell, E. Predazzi and O.V. Selyugin. High-energy hadron spin-flip amplitude at small momentum transfer and new A_v data from RHIC. EPJ A 10012-2 (2004). arxiv:hep-ph/0401040v1
14. O.V. Selyugin, J.R. Cudell, Odderon, HEGS model and LHC data. Acta Phys. Polon. Supp. **12**, 4 (2019). arxiv:1512.05130v1
15. O. V. Selyugin, High energy hadron spin flip amplitude. Phys. Part. Nucl. Lett. **13** 3, 303 (2016). arxiv:1512.05130v1
16. B.Z. Kopeliovich, M. Krelina, I.K. Potashnikova, Probing the Pomeron spin structure with Coulomb-nuclear interference. Phys. Lett. B **816**, 136262 (2021). arxiv:1910.04799v3
17. O.V. Selyugin, Nucleon structure and spin effects in elastic hadron scattering. Symmetry **13**, 164 (2021). arXiv:2012.08891v3 [hep-ph]
18. M.V. Galynskii, E.A. Kuraev, Alternative way to understand the unexpected result of JLab polarization. Phys. Rev. D **89**, 054005 (2014). arxiv:1312.3742v3
19. TOTEM Collaboration, G. Antchev et al. Proton-proton elastic scattering at the LHC energy of $\sqrt{s}$=7 TeV. EPL **95** 41001 (2011). arxiv:1110.1385v1
20. TOTEM Collaboration, G. Antchev et al. First measurement of the total proton-proton cross-section at the LHC energy of $\sqrt{s}$= 7 TeV. EPL **96**, 21002 (2011). arxiv:1110.1395v1
21. TOTEM Collaboration, G. Antchev et al. Measurement of proton-proton elastic scattering and total cross-section at $\sqrt{s}$ = 7 TeV. EPL **101**, 21002 (2013) (**CERN-PH-EP-2012-352.pdf**)
22. TOTEM Collaboration, G. Antchev et al. Luminosity-independent measurements of total, elastic and inelastic cross-section at $\sqrt{s}$= 7 TeV, EPL **101**, 21004 (2013) (**CERN-PH-EP-2012-353.pdf**)

23. TOTEM Collaboration, G. Antchev et al. Luminosity- independent measurements of proton-proton total cross section at $\sqrt{s}$ = 8 TeV. Phys. Rev. Lett. **111**, 012001 (2013) (**CERN-PH-EP-2012-354**)
24. TOTEM Collaboration, G. Antchev et al. Evidence for Non-Exponential elastic proton-proton differential cross section at low $|t|$ and $\sqrt{s}$=8 TeV. Nucl. Phys. **B899**, 527 (2015). arxiv:1503.08111v4
25. TOTEM Collaboration, G. Antchev et al. Measurement of elastic pp scattering at $\sqrt{s}$ = 8 TeV in the Coulomb – Nuclear interference region – determination of the ρ parameter and the total cross section. Eur. Phys. J. **C76**, 661 (2016). arxiv:1610.00603v1
26. TOTEM Collaboration, G. Antchev et al. First measurement of elastic, inelastic and total cross section at $\sqrt{s}$=13 TeV by TOTEM and overview of cross section data at LHC energies. Eur. Phys. J. C **79**, 103 (2019). arxiv:1712.06153v2
27. TOTEM Collaboration, G. Antchev et al. First determination of the ρ parameter at $\sqrt{s}$=13 TeV: Probing the existence of a colourless C-odd three-gluon compound state. Eur. Phys. J. C **79**, 785 (2019). arxiv:1812.04732v1
28. TOTEM Collaboration, G. Antchev et al. Elastic differential cross-section measurement at $\sqrt{s}$=13 TeV by TOTEM. Eur. Phys. J. C **79**, 861 (2019). arxiv:1812.08283v1
29. TOTEM Collaboration, G. Antchev et al. Elastic differential cross-section at $\sqrt{s}$ = 2.76 TeV and implications on the existence of a colorless 3-gluon bound state. Eur. Phys. J. **C80**, 91 (2020). arxiv:1812.08610v1
30. Y. Hagiwara, Y. Hatta, R. Pasechnik, J. Zhou, Spin-dependent Pomeron and Odderon in elastic proton-proton scattering. EPJC **80**, 427 (2020). arxiv:2003.03680
31. P. Lebiedowicz, O. Nachtmann, A. Szczurek, Central exclusive diffractive production of $K^+K^-K^+K^-$ via intermediate $\phi\phi$ state in proton-proton collisions. Phys. Rev. D **99**, 094034 (2019)
32. P. Lebiedowicz, O. Nachtmann, A. Szczurek, Searching for the odderon in $pp \to ppK^+K^-$ and $pp \to pp\mu^+\mu^-$ reaction in the $\phi(1020)$ resonance region at the LHC. Phys. Rev. D **101**, 094012 (2020)
33. R.A. Janik, J. Wosiek, Phys. Rev. Lett. **82**, 1092 (1999)
34. J. Bartels, L.N. Lipatov, G.P. Vacca, Phys. Lett. B **447**, 178 (2000)
35. L. Łukaszuk, B. Nicolescu, Lett. Nuovo Cim. **8**, 405 (1973)
36. E. Martynov, B. Nicolescu. Did TOTEM experiment discover the Odderon Phys. Lett. **B778**, 414 (2018). arxiv:1711.03288v6
37. E. Martynov, B. Nicolescu. Evidence for maximality of strong interactions from LHC forward data. **B786**, 207 (2018). arxiv:1804.10139v3
38. E. Martynov, B. Nicolescu. Odderon effects in the differential cross-sections at Tevatron and LHC energies. EPJ C **79**, 461 (2019). arxiv:1808.08580v3
39. T. Csörgő, T. Novák, R. Pasechnik, et al., Evidence of Odderon-exchange from scaling properties of elastic scattering at TeV energies. Eur. Phys. J. C **81**, 180 (2021). arXiv:1912.11968v3
40. V.M. Abazov et al., Comparison of pp and $\bar{p}p$ differential elastic cross sections and observation of the exchange of a colorless C-odd gluonic compound, FERMILAB-PUB-20-568-E, CERN-EP-2020-236. arxiv:2012.03981v1
41. T. Csörgő, I. Szanyi, Observation of Odderon Effects at LHC energies—a real extended Bialas-Bzdak model study. Eur. Phys. J. C **81**, 611 (2021). arxiv:2005.14319v3
42. G. Auberson, T. Kinoshita, A. Martin, Phys. Rev. D **3**, 3185 (1971)
43. https://pdg.lbl.gov/2017 ; C. Patrignani et al. (Particle Data Group), Chin. Phys. C **40**, 100001 (2016) and 2017 update. https://pdg.lbl.gov/2017/hadronic-xsections/hadron.html
44. https://www.hepdata.net (the old version of the Data Base is available at http://hepdata.cedar.ac.uk)